Probing ultrafast nonequilibrium dynamics in single-crystal SiC through surface nanostructures induced by femtosecond laser pulses

Wanlin He, and Jianjun Yang

Citation: Journal of Applied Physics **121**, 123108 (2017); doi: 10.1063/1.4979204
View online: https://doi.org/10.1063/1.4979204
View Table of Contents: http://aip.scitation.org/toc/jap/121/12
Published by the American Institute of Physics

Probing ultrafast nonequilibrium dynamics in single-crystal SiC through surface nanostructures induced by femtosecond laser pulses

Wanlin He[1] and Jianjun Yang[1,2,a)]
[1]*Institute of Modern Optics, Nankai University, Tianjin 300071, People's Republic of China*
[2]*Changchun Institute of Optics, Fine Mechanics and Physics, Chinese Academy of Sciences, Changchun 130033, China*

(Received 7 December 2016; accepted 14 March 2017; published online 28 March 2017)

Ultrafast non-equilibrium dynamics on the surface of a 4H-SiC crystal is experimentally investigated with time-delayed copropagating two femtosecond laser pulse trains of different linear polarizations. Rippled nanostructures are produced by this irradiation, and the alignment "slant" angle of the ripples is related to the polarizations. With varying time delays between the two laser pulses, this slant angle is found to change. In the first 10 ps, the slant quickly rotates in the direction associated with the polarization of the second incident laser pulse, but then abruptly freezes to a steady offset angle. A physical model is proposed to explain the underlying mechanisms. The first laser pulse produces a transient grating-like modulation of the dielectric constant on the surface, with which the second laser pulse interacts. Because competing fast (Auger) and slow (thermal) relaxation processes reduce the initially induced grating's dielectric constant difference, the vector sum of this partially evolved grating with the second laser pulse's interaction results in the observed slant rotation time dependence. This experiment is straightforward, conceptually simple, and utilizes commercial equipment. The time-resolved slanting of the ripple orientation provides an alternative description of the spatiotemporal evolution of a superheated semiconductor surface. *Published by AIP Publishing*. [http://dx.doi.org/10.1063/1.4979204]

I. INTRODUCTION

Ultrafast dynamic responses of materials irradiated by femtosecond laser pulses have been intensively studied for several decades. There is great interest in both the fundamental science and in broad industrial applications such as micro- to nanometer-scale precision in materials processing and manufacture. For band-gap materials, femtosecond laser-matter interaction is a very complex process, involving the generation of free carriers, the relaxation of carrier density and temperature, and various structural changes.[1–3] These non-equilibrium dynamic processes have been already investigated with several pump-probe experimental techniques, including transient reflectivity/transmission measurements,[4–6] time-resolved microscopy,[7] femtosecond electron or X-ray diffraction,[8,9] and surface plasmon resonance.[10–12] In these methods, the pump laser pulse often produces an extremely small change in the material optical properties, generating very weak intensity modulation of the probe signal. In general, there are several features these studies have in common. First, sophisticated instrumentation is required for detection with a high signal-to-noise ratio. Second, the optical changes induced by the pump laser can make a full recovery after ultrafast relaxation processes, with no damage to the material. And finally, the underlying physics is attributed to the temporal evolution of the carrier density and its induced dielectric permittivity changes, while little information is given about the transient optical effects in the spatial domain.

When the incident femtosecond laser fluence is increased to values close to the damage threshold of the material, a periodic array of subwavelength grating-like structures, or so-called ripples, can be formed on the sample surface. This phenomenon has been observed in a variety of materials such as metals,[13–15] semiconductors, and dielectrics.[16–22] In particular, using a silicon carbide (SiC) semiconductor, some authors pointed out that the formation of ripple structures was influenced by the initial surface roughness,[23] and the underlying mechanisms can be explained by a parametric decay model.[24] The observed ripple orientation dependence on laser polarization indicates the role of surface waves. It can be understood that when the spatially fringe-like laser energy deposition patterns triggered by surface wave excitations have high enough energy to exceed material deformation thresholds, the periodic grooves can be permanently imprinted on the material surface. Therefore, modifying the ultrafast surface wave excitation by the material properties can alter the formation of periodic ripple surface structures, or vice versa. By using two temporally delayed femtosecond laser pulses with either parallel or orthogonal polarizations, several authors have demonstrated controllable ripple periodicity on the semiconductors.[25,26] Ripples perpendicular to the direction of the vectorial superposition of the polarization directions of both beams were reported on a titanium surface.[27] Manipulating surface features with laser light holds promise to enhance materials processing and manufacture, but a comprehensive understanding of this issue still remains a challenge.

The previous studies have reported that the excitation of surface waves is very sensitive to the spatial patterns of the dielectric permittivities on surfaces,[28–31] whose modulations can take place in both the intensity and the direction. In this

a)Electronic mail: jjyang@nankai.edu.cn

work, we employ two sequential copropagating femtosecond laser pulse trains linearly polarized in different directions to sensitively study ultrafast spatiotemporal carrier density dynamics in a 4H-SiC crystal. The orientation of the ripple nanostructures is found to change with time delay. This method is straightforward for sensitively probing the ultrafast evolution of a superheated semiconductor material surface, in contrast to the sophisticated instrumentation required for time-resolved spectroscopy. Our theoretical analysis suggests that a transient grating-like distribution of the index is created by the first femtosecond laser pulse, which significantly affects the interaction with the second pulse. The direction of surface wave excitation of the delayed pulse is altered, resulting in a slanting of the resultant groove structure. This changeable surface wave excitation is a probe of the ultrafast spatiotemporal evolution of transient optical properties in the semiconductor. Our observations support the interference model of laser-induced periodic surface structures, giving insight into the fundamentals of femtosecond laser-matter interactions. It suggests an attractive possibility of actively controlling structure fabrication through transient surface properties of materials.

II. EXPERIMENTAL

A schematic diagram of the experimental setup is shown in Fig. 1. A commercial chirped pulse amplified Ti:sapphire laser system (Spectra Physics HP-Spitfire 50) was used, delivering a horizontally polarized train of 50 fs pulses at 1 kHz repetition rate at a central wavelength $\lambda = 800$ nm and maximum pulse energy of 2 mJ. The laser intensity profile was Gaussian. In the experiment, each output laser pulse from the amplifier was divided into two identical sub-pulses (P_1 and P_2) through a beam splitter (BS). In the optical path of P_1, an adjustable delay line was included to enable delays Δt of 0–100 ps between the two pulses, and a half-wave plate enabled linear polarization axis rotation. The two noncollinear polarization pulse trains were combined into conjoint propagation and focused in air at normal incidence onto the sample surface through a 4×, N.A. = 0.1 microscope objective lens. A single-face polished 1 mm thick crystal of 4H-SiC (001) was selected as a sample because of its unique properties and potential applications in high temperature electronic devices. The sample was placed approximately 300 μm in front of the focus, giving a calculated 1/e Gaussian laser spot diameter of approximately 60 μm. The experiments were performed by translating the sample at a speed of 0.1 mm/s resulting in 600 laser pulses partially overlapped within one beam spot area. Before and after the experiments, the sample surface was ultrasonically cleaned in acetone solution. The surface morphology was observed with a scanning electron microscope (SEM).

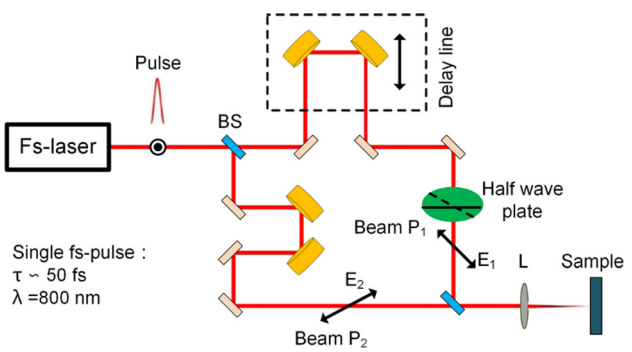

FIG. 1. Schematic diagram of the experimental setup. Abbreviations: BS: beam splitter (non-polarizing); fs: femtosecond; E_1: electric field of P_1; E_2: electric field of P_2; τ: pulse width; λ: center wavelength; L: microscope objective lens.

III. RESULTS AND DISCUSSION

First, surface morphologies of the sample irradiated by two individual femtosecond laser pulse beams were investigated at a peak fluence $F = 0.28$ J/cm^2 [Note: the threshold laser fluence was measured to be $F = 0.14$ J/cm^2], and the intersection angle θ between the two laser linear polarizations was 45°, as shown in Figs. 2(a) and 2(b). In each case, periodic ripple structures were found in the laser-exposed surface regions, with identical periodicities Λ of approximately 150 nm and the spatial orientations, respectively, perpendicular to the laser polarization directions, very similar to previous observations.[32–35] When we attenuated each laser pulse fluence to $F = 0.12$ J/cm^2, no ripples were formed. However, when these weaker trains were combined and overlapped simultaneously ($\Delta t = 0$ ps) onto the sample surface, periodic ripple structures reappeared, as shown in Fig. 2(c). Remarkably, in this case the spatial orientation of the ripple structures was neither perpendicular nor parallel to either of the two laser polarization directions, in line with the observations using a cross-polarized double-pulse trains on a titanium surface.[27] Because Λ is in the hundreds of nanometers, ripple formation cannot be attributed to interference fringes of the two laser pulses. Relative to the ripple orientation induced by P_2 in Fig. 2(b), the combined-beam ripples have a slant angle α of 25°, approximately half the intersection angle between the two laser polarizations. Ripple orientation here is clearly determined by both femtosecond laser pulse trains rather than by either one individually. The width of the swath scribed by two spatially overlapped beams was approximately 30 μm, and the ripple orientation across the entire region was found to slant in the same way, independent of the intensity variations within the Gaussian spot.

When the polarization direction of P_1 was varied, the ripple orientation also changed but still maintained at approximately half the intersection angle between the two laser polarizations, as shown in Fig. 2(d). As the polarizations approach orthogonality, ripples are no longer formed. Instead some nanoparticles begin to appear in the laser-exposed surface region. This can be attributed to the laser pulses combining to produce a circular or elliptical polarization irradiating the sample surface, which has been confirmed by a previous report.[36] When the two laser pulses are linearly polarized in the same direction, the ripples remain perpendicular to the laser polarization regardless of either scanning speeds (within a range of 0.01–0.4 mm/s) or interpulse time delay, suggesting that the varying overlap of pulses is not important in ripple slant.

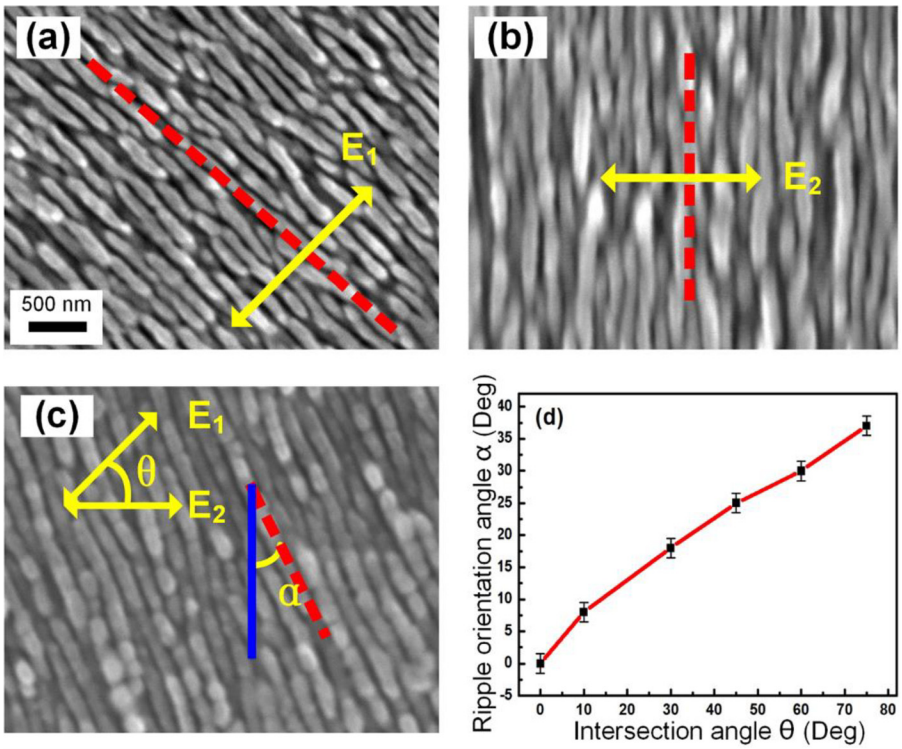

FIG. 2. (a) and (b) SEM images of the periodic ripple nanostructures formed on a 4H-SiC crystal surface by two individual femtosecond laser pulse trains. Each laser peak fluence F is 0.28 J/cm^2; (c) Ripple structures produced by two copropagating pulse with zero time delay, where each laser peak fluence F is 0.12 J/cm^2, and the intersection angle of the two laser polarizations θ is 45°. The yellow double arrows (E_1 and E_2) denote electric fields (or polarization directions) of the two laser pulse trains, while the red dashed lines represent orientations of the ripple structures. (d) Plot of the measured ripple slant versus the polarization intersection angle.

In the next series of experiments, the polarization intersection angle θ was fixed at 45° with P_2 horizontal, and the time delay was varied, P_1 leading P_2. Figure 3 shows SEM images of the ripple surface structures at various delays. The slant angle α clearly changes. Starting at $\alpha = 25°$ for $\Delta t = 0$ ps, the slant becomes 23° at $\Delta t = 2$ ps. The slant decreases rapidly to 18.3° at $\Delta t = 10$ ps, but quickly stalls at 18° for $\Delta t = 20$ ps, remaining at 18° out to delays as large as 100 ps. Beyond 100 ps, no ripple structures are formed on the semiconductor surface. At 0.12 J/cm^2, each pulse train is sub-threshold for forming ripples. Hence past 100 ps, the transient conditions set up by the first pulse have fully decayed and the two pulses are acting independent of each other.

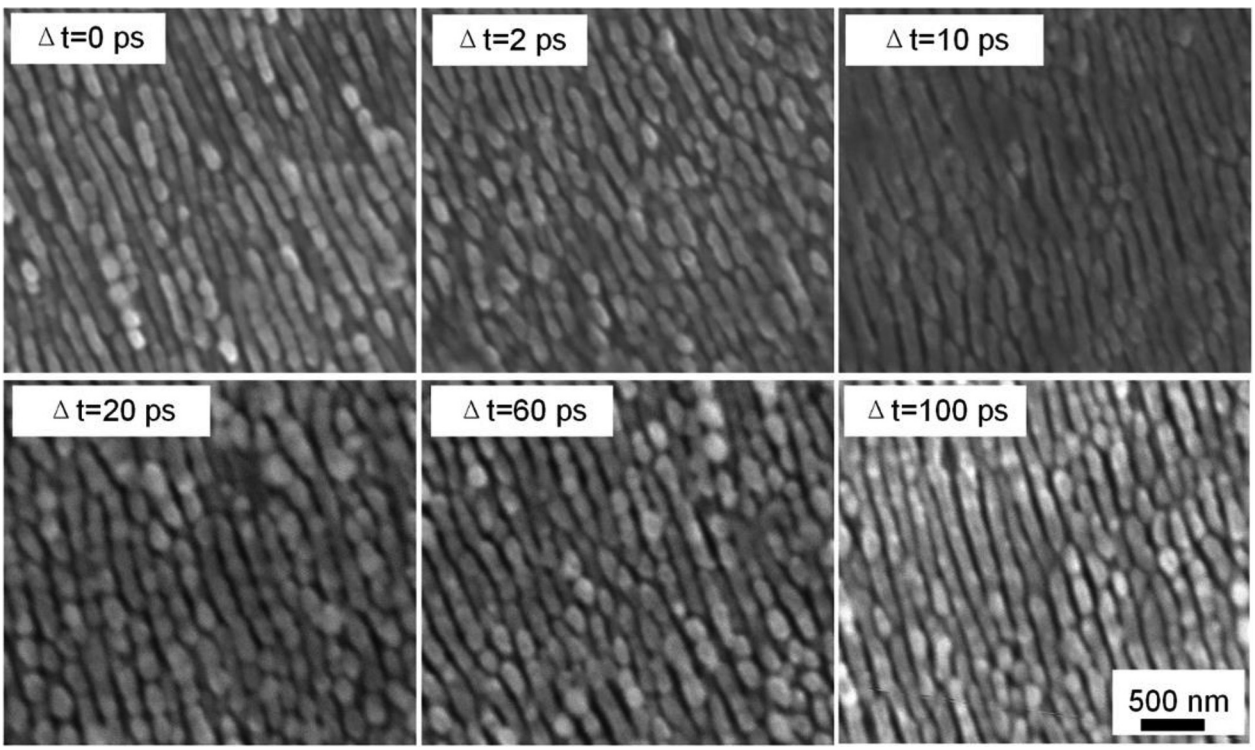

FIG. 3. Observed slanting ripple structures on 4H-SiC surfaces after irradiation with two femtosecond laser pulse trains with different time delays. The intersection angle θ is 45°, and the linear polarization of the second pulse P_2 is maintained in the horizontal direction.

Results of this experiment are shown in Fig. 4(a). Clearly, during short delays Δt of 0–20 ps, the ripple slant angle dramatically decreases, but quite abruptly it only changes very slowly in a flat profile for longer time delays, which is much different from observations in metal targets.[37] Interestingly, when the polarization intersection angle θ was changed to other values such as 10°, 30°, and 60°, very similar ripple slant time delay dependence was observed, shown in Figs. 4(b)–4(d), but the magnitudes of these shifts appear to be much different. For example, at $\theta = 10°$, the maximum ripple slant is about $\alpha = 8°$, and the values in the flattened tail are near $\alpha = 4.5°$. At $\theta = 60°$, the slant is reduced from the maximum $\alpha = 30°$ to 27° in the tail. We can understand that for a given time delay, the ripple orientation is more likely to slant away from the vertical direction when the two laser polarizations have larger intersection angles. This indicates that the formation of the slanting ripple structures is related to transient surface properties excited by the first laser pulse. The data of Fig. 4 were successfully fitted to an exponential function $\alpha \sim \exp(-t/\Delta t_1)+M$, where Δt_1 represents a surface excitation decay time constant and M an offset value. These fit parameters are $\Delta t_1 = 6.6$ ps and $M = 18.2°$ at $\theta = 45°$, $\Delta t_1 = 7.6$ ps and $M = 4.42°$ at $\theta = 10°$, $\Delta t_1 = 6.2$ ps and $M = 13.4°$ at $\theta = 30°$, and $\Delta t_1 = 6.1$ ps and $M = 27.1°$ at $\theta = 60°$.

We propose a description of the underlying physics. For single-beam femtosecond irradiation, it is known that periodic ripple surface structures are formed from the redistribution of the incident laser energy by the excited surface plasmon wave, resulting in fringe-like energy concentrations. Accordingly, for the zero-time-delay irradiation of two femtosecond laser pulses on the same surface location, two surface plasmon waves are simultaneously excited, with propagation vectors parallel to the two laser polarizations. The sum vector propagates in a direction dependent on the contributions of the two components. If the magnitudes of the two plasmon waves are identical, the vector sum is oriented along the bisector of the polarization intersection angle, giving rise to a ripple slant of $\theta/2$. Otherwise, the ripple slant deviates from $\theta/2$, which always happens in practice. This interpretation agrees well with the experimental observations in Fig. 2.

As for the evolution of the measured slant with time delay between the two pulses, we need insight into the physical dynamics of irradiated semiconductor surfaces. First, pulse P_1 creates a high-density free-electron plasma on the semiconductor surface via multiphoton absorption.[38] Under such circumstances, the interference between the surface wave and the incident light can channel the Gaussian-profiled energy into fringe-like depositions, which impose periodic modulation of the surface optical properties.[39] Consequently, a transient index grating is created with the grating vector $\boldsymbol{k}_g$ parallel to P_1's polarization. Second, during the surface relaxation processes, pulse P_2 is incident and couples to that grating. As the two laser pulses are linearly polarized in different directions, we can define an azimuth angle

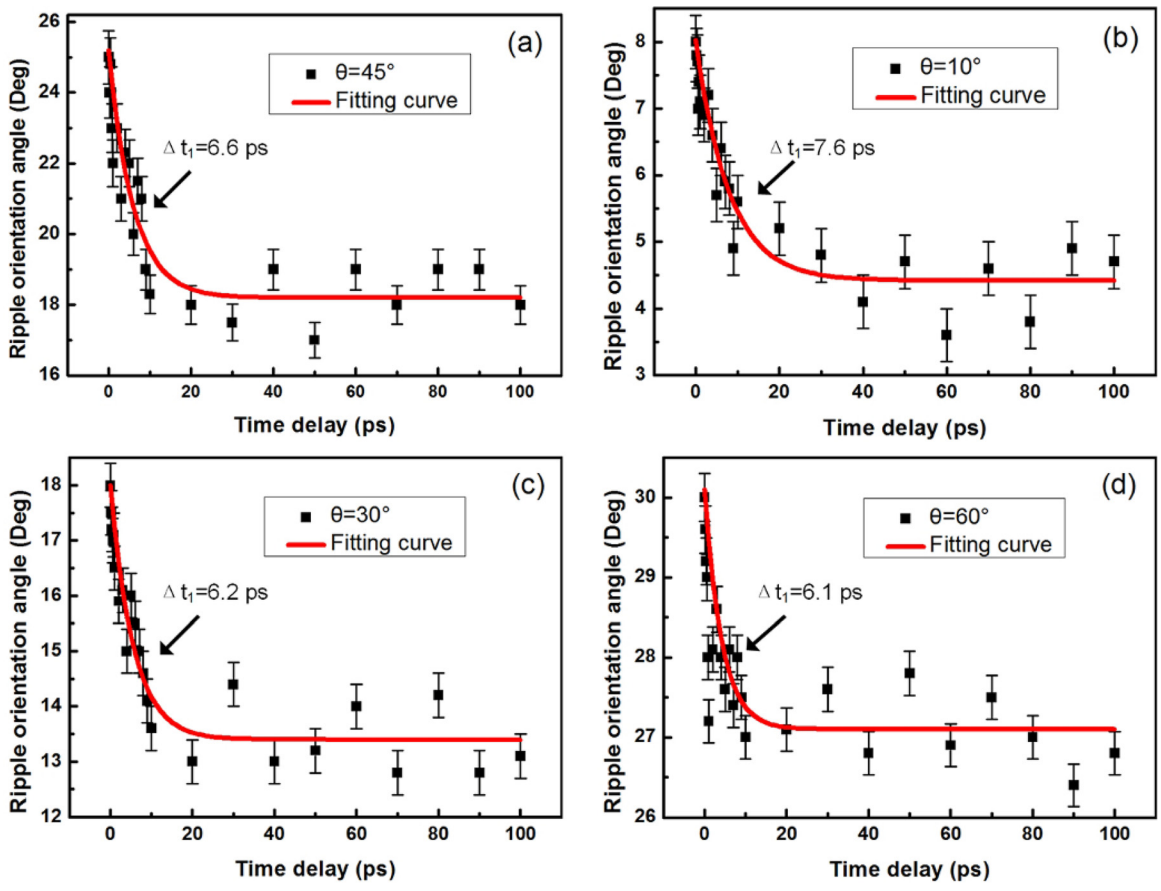

FIG. 4. Time dependence of the ripple slant angle for several laser polarization intersection angles. (a) $\theta = 45°$; (b) $\theta = 10°$; (c) $\theta = 30°$; (d) $\theta = 60°$. The fit curves (red) are exponential decays to steady offset values.

between the electric field of the delayed laser pulse and the transient index grating, which is equal to the intersection angle between the two laser polarizations. The wave vectors of the second laser pulse and the transient grating vector are not aligned, as shown in Fig. 5. Therefore, the surface wave generated by P_2 can be described by the following equations:[40]

$$k_{sw}^{delay} = \sqrt{k_{i2}^2 + k_g^2 + 2k_{i2}k_g \cos\theta}, \tag{1}$$

$$\tan\alpha = \frac{k_g \sin\theta}{k_{i2} + k_g \cos\theta}, \tag{2}$$

where $\boldsymbol{k}_{i2}$ is the wave vector of P_2. Clearly, the direction of this surface wave, with a slant α relative to P_2's polarization, is strongly dependent on the transient grating vector $\boldsymbol{k}_g$, which changes with time delay. Combining Eq. (2) with the experimental data in Fig. 4, we calculate the time delay dependence of the transient grating vector for different P_1 polarization directions, and the results are shown in Fig. 6(a). In general, the ratio k_g/k_{i2} shows a rapid decrease only for a short time of 0–10 ps, keeping steady thereafter. At a given time delay, the calculated ratio is seen to vary for different polarization intersection angles θ.

Because the transient index grating can be considered a composite layer system, its effective real part of the dielectric constant ε_{eff} is obtained by[41]

$$\varepsilon_{eff} = \varepsilon_1 \left[\frac{\varepsilon_2 + 2\varepsilon_1 + 2f(\varepsilon_2 - \varepsilon_1)}{\varepsilon_2 + 2\varepsilon_1 - f(\varepsilon_2 - \varepsilon_1)}\right], \tag{3}$$

where $\varepsilon_1 = 7.69$ (at 800 nm) is the real part of the dielectric constant for the equilibrium state, ε_2 is the same for the optically excited region of the sample surface, and f is the overlapping volume fraction. According to previous studies,[13,15,22] although the imaginary part of the dielectric constant of semiconductor materials can also change with excitation from femtosecond laser pulses, representing modulations in absorption, its physical role in ripple orientation is usually neglected. If $\Delta\varepsilon = \varepsilon_2 - \varepsilon_1$ is the change in the real part of dielectric constant for the transient index grating, the above equation can be rewritten as

$$\Delta\varepsilon = \frac{-3\varepsilon_1}{1 - f - 3f\left(\frac{\varepsilon_1}{\varepsilon_{eff} - \varepsilon_1}\right)}. \tag{4}$$

The term $\varepsilon_{eff} - \varepsilon_1$ represents the change of the real part of the dielectric constant before and after the femtosecond laser irradiation, i.e., an additional dielectric constant provided by the transient index grating. $\Delta\varepsilon$ will be zero when $\varepsilon_{eff} = \varepsilon_1$, indicating the disappearance of the grating. When the grating is present, usually $\varepsilon_{eff} < \varepsilon_1$, so the quantity $(\varepsilon_{eff} - \varepsilon_1)$ can be replaced by $-(k_g/k_{i2})^2$. Therefore, a modification of Eq. (4) is

$$\Delta\varepsilon = \frac{-3\varepsilon_1}{1 - f + 3f\frac{\varepsilon_1}{(k_g/k_{i2})^2}}. \tag{5}$$

Using Eq. (5) we obtained the temporal evolution of $\Delta\varepsilon$ on the irradiated semiconductor surface following pulse P_1. As shown in Fig. 6(b), for a specified volume fraction f of 0.5, $\Delta\varepsilon$ changes sharply from large to small negative values in the initial 10 ps and then stays effectively unchanged for longer time delays. As discussed in previous studies,[42,43] in semiconductors Auger recombination plays an important role in reducing the number of laser-generated conduction band electrons at the surface, resulting in a rapid dramatic change in the delay dependence of the dielectric constant. The weaker but steady negative contributions at longer time delays arise from elevated lattice temperature caused by energy transfer via electron-phonon coupling. For the derived $\Delta\varepsilon$ data at $\theta = 45°$, 30°, and 60°, the exponential fit decay times are 6.1 ps, 5.6 ps, and 5.4 ps. These values are very similar to the ones obtained from Fig. 4. The maximum $\Delta\varepsilon$ values decrease with larger polarization intersection angles θ. This effect can be attributed to the polarization-dependent optical absorption of femtosecond laser pulses in crystalline materials,[44] which results in both density and temperature differences in the free-electron plasma in semiconductors. This can explain some variation in ripple slant as the direction of P_1's polarization was changed. Figure 6(c) shows the $\Delta\varepsilon$ time dependence for several different values of the volume overlap fraction f with fixed angle θ. Smaller volume fractions require larger negative values of $\Delta\varepsilon$, substantially so for small f.

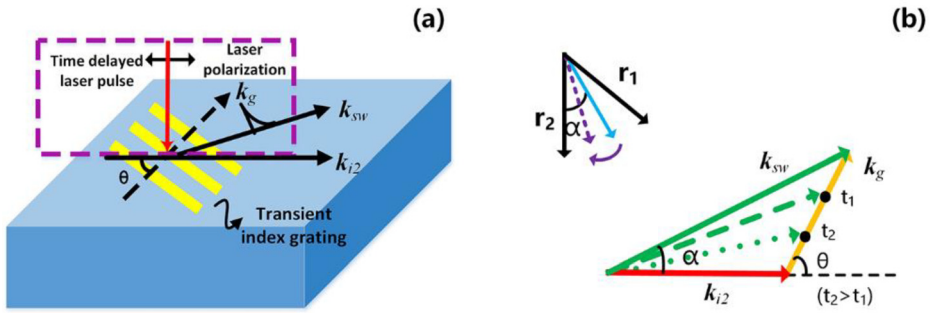

FIG. 5. Proposed physical model for ripple slant upon irradiation with two sequential femtosecond laser pulses. (a) Diagram of the ultrafast physical processes occurring on the semiconductor surface. A spatially periodic change of the optical index is created by the first laser pulse, which affects the surface wave excitation induced by the second pulse. The combined interaction causes the ripple slant to deviate from either pulse's polarization direction; (b) A vector diagram for the direction of the surface wave excitation (k_{sw}) when the delayed pulse (k_{i2}) is coupled with the transient grating vector (k_g) at different time delays ($t_2 > t_1$). The ripple orientations induced by the two pulses P_1 and P_2 are denoted by r_1 and r_2.

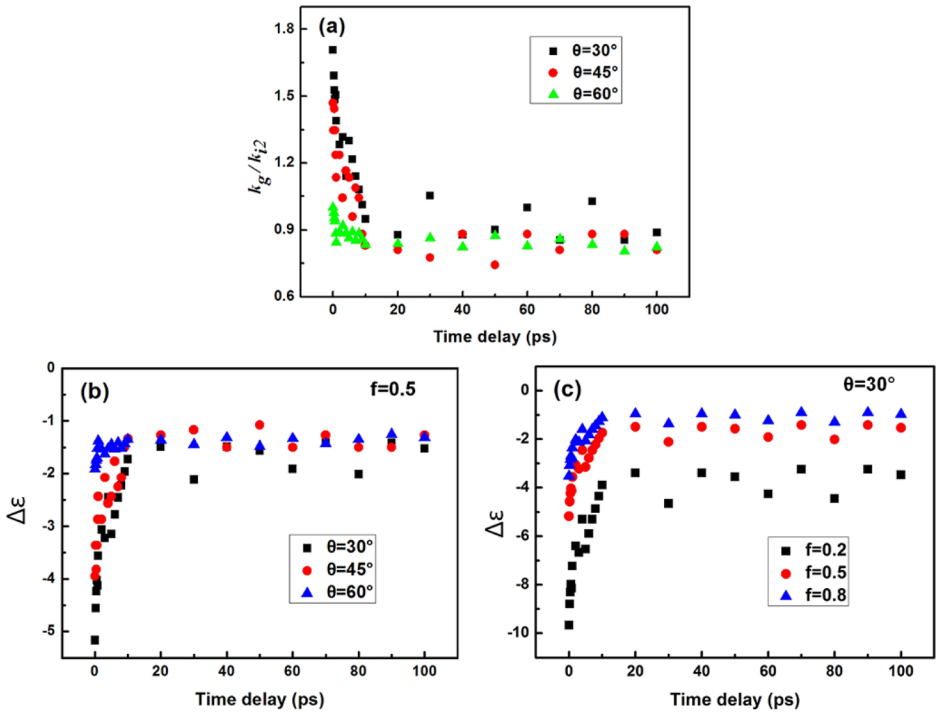

FIG. 6. Derived time dependence of transient physical properties on the semiconductor surface excited by the first femtosecond laser pulse. (a) Ratio of the transient grating vector to the laser wavelength k_g/k_{i2}; (b) Variation of the real part of dielectric constant $\Delta\varepsilon$ for polarization intersection angles θ of 30°, 45°, and 60°; (c) $\Delta\varepsilon$ for f values of 0.2, 0.5, and 0.8.

Fundamentally, the emergence of a transient index grating begins with the intensity fringes and their subsequent optical heating. Some periodically distributed surface regions in the beam develop a high temperature free-electron plasma, while other regions remain in equilibrium. The variation of the dielectric constant is concentrated in the excited regions. Compared with metal targets, the thermal conductivity in semiconductors is relatively poor; thus, the high temperature of the periodic surface regions decreases slowly. Energy diffusion in semiconductor surfaces is weak. This ensures long-term sustainability of the transient index grating, which is what is seen in the experiments as the long flat temporal tail of the ripple slant angle. In metals, the slant can rapidly decrease to zero in less than 40 ps, without displaying any flattening of the curve.[37] Dramatic reduction in the slant angle indicates a strong change of the dielectric constant in the sample surface, while the long flat tail indicates the sustainability of the transient index grating.

The evaluated dielectric constant variation $\Delta\varepsilon$ in the transient grating is relatively small, indicating that the excited dielectric constant could possibly be positive. Under such circumstances, the surface dielectric constant may not directly support surface plasmon production, because $\Delta\varepsilon$ comes about from the first femtosecond pulse, leading to no permanent ripple structures. In this situation, it is only the second laser pulse that sends the dielectric constant negative, resulting in the ripple structures.

IV. CONCLUSIONS

We have investigated ultrafast dynamics in the semiconductor 4H-SiC by observing the laser-induced periodic surface ripple structures using two copropagating 1-kHz, 800-nm, 50-fs laser-pulse trains of different linear polarizations. We found that the slanted orientation of the ripple structures changes as the time delay between the two laser pulses is varied. Interestingly, the ripple slant undergoes a rapid decrease for the first 10 ps, followed by an abrupt transition to a steady value. This is observed for several different intersection angles between the two laser polarizations. Analysis of the experimental results leads us to consider the nonequilibrium processes in an optically excited semiconductor surface. Irradiation by the first femtosecond pulse produces a grating-like profile of optical index change via surface plasmon excitation. The temporal relaxation of such a transient index grating affects the direction of the surface wave excitation brought about by the second laser pulse, and consequently the directions of the resultant ripples. These theoretical interpretations are consistent with the experimental observations. We have derived the time evolution of both the grating vector and the dielectric constant in the transient surface grating. Our investigations give a method to sensitively probe ultrafast dynamic processes in superheated materials without sophisticated instrumentation, of benefit to the understanding of femtosecond laser-matter interactions for active control of nanostructure fabrication.

ACKNOWLEDGMENTS

The authors acknowledge financial support for this work provided by the Natural National Science Foundation of China (NSFC) through Grant Nos. 11274184 and 11674178, the Tianjin National Natural Science Foundation Grant No. 12JCZDJC20200, and the Research Fund for the Doctoral Program of Higher Education of China Grant No. 20120031110032.

[1]R. R. Gattass and E. Mazur, Nat. Photonics **2**, 219 (2008).
[2]B. C. Stuart, M. D. Feit, A. M. Rubenchik, B. W. Shore, and M. D. Perry, Phys. Rev. Lett. **74**, 2248 (1995).
[3]A. Kaiser, B. Rethfeld, M. Vicanek, and G. Simon, Phys. Rev. B **61**, 11437 (2000).

[4]E. N. Glezer, Y. Siegal, L. Huang, and E. Mazur, Phys. Rev. B **51**, 6959 (1995).
[5]H. W. K. Tom, G. D. Aumiller, and C. H. Brito-Cruz, Phys. Rev. Lett. **60**, 1438 (1988).
[6]D. Puerto, W. Gawelda, J. Siegel, J. Bonse, G. Bachelier, and J. Solis, Appl. Phys. A **92**, 803 (2008).
[7]K. Sokolowski-Tinten, J. Bialkowski, A. Cavalleri, D. von der Linde, A. Oparin, J. Meyer-ter-Vehn, and S. I. Anisimov, Phys. Rev. Lett. **81**, 224 (1998).
[8]B. J. Siwick, J. R. Dwyer, R. E. Jordan, and R. J. Dwayne Miller, Science **302**, 1382 (2003).
[9]A. Rousse, C. Rischel, S. Fourmaux, I. Uschmann, S. Sebban, G. Grillon, Ph. Balcon, E. Förster, J. P. Geindre, P. Audebert, J. C. Gauthier, and D. Hulin, Nature **410**, 65 (2001).
[10]R. H. M. Groeneveld, R. Sprik, and Ad. Lagendijk, Phys. Rev. Lett. **64**, 784 (1990).
[11]A. Devižis and V. Gulbinas, Appl. Opt. **47**, 1632 (2008).
[12]J. Wang and C. Guo, Phys. Rev. B **75**, 184304 (2007).
[13]A. Y. Vorobyev, V. S. Makin, and C. Guo, J. Appl. Phys. **101**, 034903 (2007).
[14]Y. Tang, J. Yang, B. Zhao, M. Wang, and X. Zhu, Opt. Express **20**, 25826 (2012).
[15]F. Garrelie, J. P. Colombier, F. Pigeon, S. Tonchev, N. Faure, M. Bounhalli, S. Reynaud, and O. Parriaux, Opt. Express **19**, 9035 (2011).
[16]A. Borowiec and H. K. Haugen, Appl. Phys. Lett. **82**, 4462 (2003).
[17]G. Miyaji, K. Miyazaki, K. Zhang, T. Yoshifuji, and J. Fujita, Opt. Express **20**, 14848 (2012).
[18]R. L. Harzic, D. Dörr, D. Sauer, F. Stracke, and H. Zimmermann, Appl. Phys. Lett. **98**, 211905 (2011).
[19]Y. Ma, V. Khuat, and A. Pan, Opt. Laser Eng. **82**, 141–147 (2016).
[20]T. J. Song, W. Tao, H. Song, M. Gong, G. Ma, Y. Dai, Q. Zhao, and J. Qiu, Appl. Phys. A **122**, 341 (2016).
[21]S. K. Das, H. Messaoudi, A. Debroy, E. McGlynn, and R. Grunwald, Opt. Mater. Express **3**, 1705 (2013).
[22]J. Bonse and J. Krüger, J. Appl. Phys. **108**, 034903 (2010).
[23]T. Takuro, K. Kinoshita, S. Matsuo, and S. Hashimoto, Appl. Phys. Lett. **90**, 153115 (2007).
[24]L. Gemini, M. Hashida, M. Shimizu, Y. Miyasaka, S. Inoue, S. Tokita, J. Limpouch, T. Mocek, and S. Sakabe, J. Appl. Phys. **114**, 194903 (2013).
[25]M. Barberoglou, D. Gray, E. Magoulakis, C. Fotakis, P. A. Loukakos, and E. Stratakis, Opt. Express **21**, 18501 (2013).
[26]X. Shi, L. Jiang, X. Li, S. Wang, Y. Yuan, and Y. Lu, Opt. Lett. **38**, 3743 (2013).
[27]M. Hashida, T. Nishii, Y. Miyasaka, H. Sakagami, M. Shimizu, and S. Inoue, Appl. Phys. A **122**, 484 (2016).
[28]W. L. Barnes, A. Dereux, and T. W. Ebbesen, Nature **424**, 824 (2003).
[29]J. A. Porto, F. J. García-Vidal, and J. B. Pendry, Phys. Rev. Lett. **83**, 2845 (1999).
[30]N. Walk, A. P. Lund, and T. C. Ralph, New J. Phys. **15**, 073014 (2013).
[31]E. Laux, C. Genet, T. Skauli, and T. W. Ebbesen, Nat. Photonics **2**, 161 (2008).
[32]S. Höhm, A. Rosenfeld, J. Krüger, and J. Bonse, J. Appl. Phys. **112**, 014901 (2012).
[33]T. Jia, H. Chen, M. Huang, F. Zhao, J. Qiu, R. Li, Z. Xu, X. He, J. Zhang, and H. Kuroda, Phys. Rev. B **72**, 125429 (2005).
[34]J. Cong, J. Yang, B. Zhao, and X. Xu, Opt. Express **23**, 5357 (2015).
[35]S. Höhm, M. Herzlieb, A. Rosenfeld, J. Krüger, and J. Bonse, Appl. Surf. Sci. **336**, 39 (2015).
[36]J. Reif, O. Varlamova, and F. Costache, Appl. Phys. A: Mater. Sci. Process. **92**, 1019–1024 (2008).
[37]B. Zhao, J. Yang, X. Zhu, X. Xu, and F. Xie, "Surface dynamics of warm dense copper metal captured in femtosecond laser-induced deflecting ripple structures," New J. Phys. (to be published).
[38]G. Obara, H. Shimizu, T. Enami, E. Mazur, M. Terakawa, and M. Obara, Opt. Express **21**, 26323 (2013).
[39]S. Höhm, A. Rosenfeld, J. Krüger, and J. Bonse, Appl. Phys. Lett. **102**, 054102 (2013).
[40]B. Tremain, H. J. Rance, A. P. Hibbins, and J. R. Sambles, Sci. Rep. **5**, 09366 (2015).
[41]R. Ruppin, Phys. Status Solidi B **87**, 619–624 (1978).
[42]S. Höhm, A. Rosenfeld, J. Krüger, and J. Bonse, Appl. Surf. Sci. **278**, 7 (2013).
[43]T. J.-Y. Derrien, J. Krüger, T. E. Itina, S. Höhm, A. Rosenfeld, and J. Bonse, Appl. Phys. A **117**, 77 (2014).
[44]M. Gertsvolf, H. Jean-Ruel, P. P. Rajeev, D. D. Klug, D. M. Rayner, and P. B. Corkum, Phys. Rev. Lett. **101**, 3382 (2008).